Calculation of Infinite-Dilution Partial Molar Properties by Computer Simulation

Partial molar properties at infinite dilution for binary Lennard-Jones mixtures are calculated using Monte Carlo simulation methods. The variation of these properties with density, temperature, and intermolecular force parameters is systematically studied. Simulation pair correlation functions are used to examine the structure of the mixtures at the molecular level. Results are also compared to predictions of the van der Waals I conformal solution theory.

Partial molar volume and internal energy are found to be strongly dependent on the isothermal compressibility of the mixture and on the proximity of the mixture state condition to phase boundaries. The van der Waals I conformal solution theory gave good results for the infinite-dilution chemical potential μ_1^∞ and reasonable results for the partial molar internal energies and volumes. However, it is suspected that this is limited to the infinite-dilution case, where the isothermal compressibility of the mixture is well represented by the pure-fluid equation of state.

Katherine S. Shing, Sang-Tae Chung
Department of Chemical Engineering
University of Southern California
Los Angeles, CA 90089-1211

Introduction

The development and testing of mixing rules have generated considerable interest in recent years. The objective is to obtain mixing rules applicable to highly nonideal mixtures over extended temperature and density ranges. If this objective can be achieved, then the equation of state approach can be used to predict not only phase equilibrium, but also enthalpies and densities. To avoid ambiguities introduced when parameters are fitted, one usually uses computer simulation data in critical evaluation of mixing rules.

An additional benefit of simulation is that it provides structural information such as correlation functions. Since many molecular-based mixing rules are postulated on the basis of structure, such structural information allows testing of the mixing rules at a microscopic, structural level. We have previously carried out mixing rule studies based on chemical potentials for Lennard-Jones mixtures at high densities (Shing and Gubbins, 1981, 1982). In this study simulation data for the partial molar enthalpies, chemical potentials, and partial molar volumes at various temperatures and pressures are generated for Lennard-Jones mixtures. To reduce the number of simulations, we consider here only the infinite-dilution binary mixture case, and calculate several partial molar properties at infinite dilution, including the chemical potential, partial molar internal energy, and partial molar volume at infinite dilution, μ_1^∞, $\bar{U}_1^\infty$, and $\bar{V}_1^\infty$, respectively. Here 1 indicates the solute and 2 the solvent. μ_1^∞ characterizes the phase equilibria or solubility; $\bar{U}_1^\infty$ and $\bar{V}_1^\infty$ characterize the temperature and pressure dependence of the solubility. Since these are derivative properties, they provide a very stringent test of the mixing rules.

Simulation of infinite-dilution partial molar properties can serve another useful purpose. We know that μ_1^∞ is related to the Henry's constants, which can be accurately determined experimentally. Recently, accurate experimental measurement of $\bar{V}_1^\infty$ has also been reported (Eckert et al., 1986). Comparison of simulated μ_1^∞ and $\bar{V}_1^\infty$ to experimental measurements will enable us to develop much better intermolecular potential models for the solute-solvent interactions. In this work, however, we restrict our attention to the use of partial molar properties in mixing rules studies.

In the case of infinitely dilute binary Lennard-Jones mixtures, two mixture parameters characterize *the properties of* the mixture, namely $\epsilon_{12}/\epsilon_{22}$ and σ_{12}/σ_{22}, where ϵ_{12} and σ_{12} are the energy and size parameters of the solute-solvent interaction, and ϵ_{22}, σ_{22} are the corresponding quantities for the solvent-solvent interaction.

Correspondence concerning this paper should be directed to K. S. Shing.

Simulation Method

μ_1^∞, Chemical potential of solute at infinite dilution

Two different methods were used to calculate μ_1^∞. At low to moderate densities, for solutes which are not too large, the test particle method based on the potential distribution theorem (Widom, 1963) is used:

$$\mu_1^{r\infty} = -kT \ln [\langle \exp(-\psi_1/kT) \rangle_2] \tag{1}$$

where

$\mu_1^{r\infty}$ is the residual chemical potential of solute at infinite dilution
ψ_1 is the energy experienced by a solute test particle
$\langle\ \rangle_2$ is a canonical ensemble average of pure solvent 2

When the density is high and/or when the solute is large, we used the Kirkwood equation as basis (Shing and Chung, 1987)

$$\mu_1^{r\infty} = \mu_2^{r0} + \int_0^1 \langle \Delta\psi_1 \rangle_\xi \, d\xi \tag{2}$$

where

μ_2^{r0} is the pure solvent residual chemical potential
$\Delta\psi_1 \equiv \psi_1 - \psi_2$, ψ_2 is the energy experienced if the solute molecule were a solvent molecule
$\langle\ \rangle_\xi$ is an isothermal-isobaric ensemble average in which the actual interaction between the solute and the rest of the solvent molecules is $\psi_2 + \xi\Delta\psi_1$; ξ is the Kirkwood charging parameter

$\bar{U}_1^\infty$, Partial molecular internal energy of solute at infinite dilution

The partial molar internal energy is defined as

$$\bar{U}_1^\infty = \lim_{N_1 \to 0} \left(\frac{\partial U}{\partial N_1}\right)_{T,P,N_2} \sim U(N_1 = 1, N_2, T, P) - U(N_1 = 0, N_2, T, P) \tag{3}$$

$U(N_1 = 1)$ is obtained from simulation and $U(N_1 = 0)$ is obtained from the Lennard-Jones equation of state (Nicolas et al., 1979). $\bar{U}_1^\infty$ is found by difference.

$\bar{V}_1^\infty$, Partial molar volume of solute at infinite dilution

$$\bar{V}_1^\infty \equiv \lim_{N_1 \to 0} \left(\frac{\partial V}{\partial N_1}\right)_{T,P,N_2} \sim V(N_1 = 1, N_2, T, P) - V(N_1 = 0, N_2, T, P) \tag{4}$$

Again $V(N_1 = 1)$ is obtained from simulation and $V(N_1 = 0)$ is found from the Lennard-Jones equation of state.

Alternative method

For mixtures at finite concentrations, an alternative simulation method based on fluctuation theory (Debenedetti, 1986) may be used to calculate $\bar{V}_1$ and $\bar{U}_1$. This method, however, cannot be used for very dilute mixtures because the solute-related fluctuations are very poorly sampled in dilute solutions. It is noted that since $\bar{U}_1^\infty$ and $\bar{V}_1^\infty$ are obtained by difference here, the numerical uncertainties may be large. The magnitudes of the uncertainties depend on the state of the mixture, the type of mixture, the size of the system, and the length of the simulation. At present, different mixing rules predict different partial molar quantities and reasonable comparisons can be made even though the uncertainties may be large. In any case, the uncertainties may be reduced, if necessary, by performing longer simulations. We will see later that comparisons of structure are less subject to the problem of large uncertainties associated with partial molar quantities such as $\bar{V}_1^\infty$ and $\bar{U}_1^\infty$. For details of the simulation methods, see the appendix.

Van der Waals I Mixing Rules

A brief comparison of the simulation results and the van der Waals I mixing rules (Leland et al., 1968) is given later to demonstrate the combined use of the partial molar properties and the distribution functions. It is convenient at this point to examine the representation of structure in the van der Waals I theory. It has been shown that the van der Waals I mixing rules

$$\sigma_x^3 = \Sigma x_i x_j \sigma_{ij}^3$$

and

$$\epsilon_x \sigma_x^3 = \Sigma x_i x_j \epsilon_{ij} \sigma_{ij}^3 \tag{5}$$

are equivalent to the approximation (McDonald, 1973)

$$g_{ij}^{\text{mixture}}\left(r, T, \frac{N}{V}\right) = g^{\text{pure}}\left(\frac{r}{\sigma_{ij}}, \frac{kT}{\epsilon_x}, \frac{N}{V}\sigma_x^3\right) \tag{6}$$

At infinite dilution of solute 1, we have

$$g_{22}\left(r, T, \frac{N}{V}\right) = g^{\text{pure}}\left(\frac{r}{\sigma_{22}}, \frac{kT}{\epsilon_{22}}, \frac{N}{V}\sigma_{22}^3\right) \tag{7}$$

$$g_{12}\left(r, T, \frac{N}{V}\right) = g^{\text{pure}}\left(\frac{r}{\sigma_{12}}, \frac{kT}{\epsilon_{22}}, \frac{N}{V}\sigma_{22}^3\right) \tag{8}$$

We note here that while we expect Eq. 7 to be a good approximation, Eq. 8, which the partial molar properties are dependent on, has several problems.

First, Eq. 8 is completely independent of ϵ_{12}. This may not be a severe problem at high densities where the structure is primarily determined by the repulsive forces, but it clearly is not valid at low densities. In particular, at the second virial limit, we know that

$$g_{12}(r, T) = \exp\left[-\frac{\phi_{12}(r)}{kT}\right] \tag{9}$$

where

$$\phi_{12} = 4\epsilon_{12}\left[\left(\frac{\sigma_{12}}{r}\right)^{12} - \left(\frac{\sigma_{12}}{r}\right)^{6}\right]$$

for the Lennard-Jones potential.

The van der Waals I mixing rules clearly do not satisfy the second virial limit. The second problem is that since the mixture distribution function g_{12} is approximated by a pure fluid distribution function, we will expect the temperature and density dependence of the approximated g_{12} to be identical to those of a

Table 1. Partial Molar Properties at $T^* = 1.2$ for Various $\epsilon_{12}/\epsilon_{22}$

	$\rho^* = 0.7$ ($p^* = 0.6545$) $\sigma_{12}^3 = 2.7\,\sigma_{22}^3$			$\rho^* = 0.6$ ($p^* = 0.0997$) $\sigma_{12}^3 = 2.0\,\sigma_{22}^3$		
$\epsilon_{12}/\epsilon_{22}$	μ_1^∞	$\bar{U}_1^\infty$	$\bar{V}_1^\infty$	μ_1^∞	$\bar{U}_1^\infty$	$\bar{V}_1^\infty$
0.02	—	—	—	—	31.8 ±2.5	14.3 ±2.0
0.1	—	—	—	7.6 ±1.5	46.0 ±7.5	25.6 ±4.6
0.2	—	—	—	6.1 ±1.1	40.2 ±5.0	21.6 ±2.5
0.4	—	—	—	2.2 ±1.0	37.8 ±3.3	22.3 ±1.9
0.5	6.18 ±1.2	11.5 ±3.0	8.1 ±1.4	1.9 ±0.8	26.6 ±2.7	16.3 ±1.6
0.6	—	—	—	—	13.8 ±2.1	11.0 ±1.4
1.0	−3.2 ±0.5	1.3 ±2.9	8.4 ±1.5	−5.64 ±0.9	−4.6 ±3.0	5.1 ±1.0
1.4	—	—	—	—	−9.5 ±2.4	5.8 ±1.5
1.5	−16.3 ±1.0	−22.9 ±4.2	4.8 ±1.1	−17.0 ±1.4	−10.4 ±2.0	5.0 ±1.8
2.0	−29.5 ±3.0	−34.8 ±2.7	4.8 ±0.8	−27.2 ±2.3	−38.8 ±3.4	−1.6 ±1.4

Uncertainties are from statistical fluctuations only; see appendix for discussion
$\rho^* \equiv \rho\sigma_{22}^3$; $p^* \equiv p\sigma_{22}^3/\epsilon_{22}$
μ_1^∞, $\bar{U}_1^\infty$ reduced with respect to ϵ_{22}
$\bar{V}_1^\infty$ reduced with respect to σ_{22}^3

pure fluid g. We will show later that this is not the case in general.

Simulation Results and Discussion

μ_1^∞, $\bar{U}_1^\infty$, and $\bar{V}_1^\infty$ were calculated for several mixtures, and effects of variation in density, temperature, and $\epsilon_{12}/\epsilon_{22}$ were studied. The results are shown in Tables 1–3 and in Figures 1, 3, and 5. Figures 1a and 1b show the effect of changing the ratio $\epsilon_{12}/\epsilon_{22}$ on the partial molar properties at a subcritical temperature $T^* = 1.2$ and at liquidlike densities. The trends shown in Figure 1 make physical sense. μ_1^∞ is positive for $\epsilon_{12}/\epsilon_{22} < 1$ and negative for $\epsilon_{12}/\epsilon_{22} > 1.0$.

The chemical potential μ_1^∞ is a measure of the reversible work done in introducing a solute particle originally at infinity into the solvent under constant temperature and pressure conditions. This reversible work can be considered to be composed of two parts:

1. The reversible work done on the solvent to create a cavity for the solute particle
2. The reversible work done by the system to reduce the increased intermolecular potential energy of the system (due to the added solute particle) in order to maintain constant temperature and pressure

When ϵ_{12} is small, the work done to create the cavity exceeds the gain in potential energy, hence μ_1^∞ is positive. Alternatively, we can say that the entropic contribution (required to perturb the solvent structure) overwhelms the energetic contribution from the solvent-solute interactions. When ϵ_{12} is large, the energetic contribution dominates the entropic contribution and the resultant μ_1^∞ is negative. $\bar{V}_1^\infty$ are rather small and positive and decrease with increasing ϵ_{12}. This is because the mixture is at liquid density and hence incompressible, and the addition of a solute molecule results in a volume increase. Increased ϵ_{12} tends to increase attraction between solute and solvent and to draw solvent molecules closer to the solute, hence a decrease in $\bar{V}_1^\infty$ with ϵ_{12}. $\bar{U}_1^\infty$ is correlated with $\bar{V}_1^\infty$ since a reduction in $\bar{V}_1^\infty$ (or a compression) causes molecules to move closer together and usually results in increased attraction or more negative $\bar{U}_1^\infty$.

Figure 1b shows similar data for a slightly lower density of $\rho^* = 0.6$. We see that the qualitative features are unchanged, except that at low ϵ_{12} we see large positive increases in $\bar{V}_1^\infty$ and $\bar{U}_1^\infty$. To explain this feature, we must take into account both the interaction between solvent and solute as well as the solvent state condition. When ϵ_{12} is small, the interaction between solute and solvent is weak. Since the σ_{12} in this case is large, the solute is acting as an insulator in the solvent medium. The effect of having a weakly interacting (small ϵ_{12}) but large solute is to separate the solvent molecules and to screen some of the interaction between the solvent molecules (which are now further apart). This results in a reduction of the cohesive energy in the system and the system tends to expand, hence the positive $\bar{V}_1^\infty$. Now the solvent state condition of $T^* = 1.2$ and $\rho^* = 0.6$ is close to the vapor-liquid coexistence curve, so the liquid is easily expandable. Consequently we see a large positive $\bar{V}_1^\infty$, which in turn gives a large and positive $\bar{U}_1^\infty$. We would like to emphasize that this expansion occurs only at the local level in the vicinity of the solute molecule and has no effect on the macroscopic or bulk

Table 2. Partial Molar Properties as Function of Density at $T^* = 1.5$

		$\epsilon_{12} = 0.5\,\epsilon_{22}$			$\epsilon_{12} = 1.5\,\epsilon_{22}$		
ρ^*	p^*	μ_1^∞	$\bar{U}_1^\infty$	$\bar{V}_1^\infty$	μ_1^∞	$\bar{U}_1^\infty$	$\bar{V}_1^\infty$
0.1	0.1166	−0.16 ±0.08	−4.3 ±1.8	21.2 ±11	−5.2 ±0.3	−17.1 ±1.5	−47.6 ±13
0.2	0.1803	−0.08 ±0.1	−2.3 ±4	26.8 ±10	−9.4 ±0.4	−52.6 ±10	−76.3 ±15
0.3	0.2208	0.5 ±0.1	−0.4 ±10	24.7 ±18	—	—	—
0.4	0.2691	1.4 ±0.3	23.9 ±11	43.9 ±12	−15.8 ±0.8	−48.0 ±15.0	−12.0 ±5
0.5	0.3784	4.6 ±0.4	23.1 ±8.2	26.0 ±6	—	—	—
0.6	0.7146	8.5 ±2.0	17.9 ±3.3	15.7 ±1.5	−18.5 ±1.0	−24.9 ±6.5	9.2 ±2.7

$\sigma_{12}^3 = 3.5\,\sigma_{22}^3$

Table 3. Partial Molar Properties as a Function of Density at $T^* = 2.0$

		$\epsilon_{12} = 0.5\,\epsilon_{22}$			$\epsilon_{12} = 1.5\,\epsilon_{22}$		
ρ^*	p^*	μ_1^∞	$\bar{U}_1^\infty$	$\bar{V}_1^\infty$	μ_1^∞	$\bar{U}_1^\infty$	$\bar{V}_1^\infty$
0.2	0.3272	1.4 ±0.2	−1.9 ±3	18.0 ±6	−7.4 ±0.5	−20.8 ±1.5	−13.3 ±3.5
0.4	0.6870	5.3 ±0.3	3.9 ±3	15.3 ±3	−11.1 ±0.5	−25.2 ±5.5	5.2 ±3.5
0.6	1.6931	16.2 ±1.6	9.8 ±3.4	11.5 ±1.5	−10.0 ±1.2	−23.0 ±3.7	9.3 ±1.2

$\sigma_{12}^3 = 3.5\,\sigma_{22}^3$

density, which for the infinitely dilute case is identical to the pure solvent density at the specified temperature and pressure. It is instructive to examine the distribution function, g_{12}, values obtained from simulation to see if they are consistent with the above explanation. In Figure 2, g_{12} curves for three different ϵ_{12} values for the system studied in Figure 1b are shown. We see indeed that when $\epsilon_{12} = 2$, g_{12} has a high peak, indicating that solvent molecules are tightly bound to the solute molecule. When $\epsilon_{12} = 0.2$, a weak peak is seen, indicating that now the weak solute is no longer able to hold solvent molecules close and

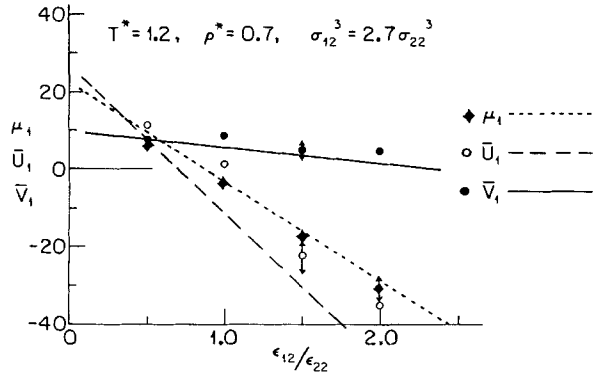

Figure 1a.

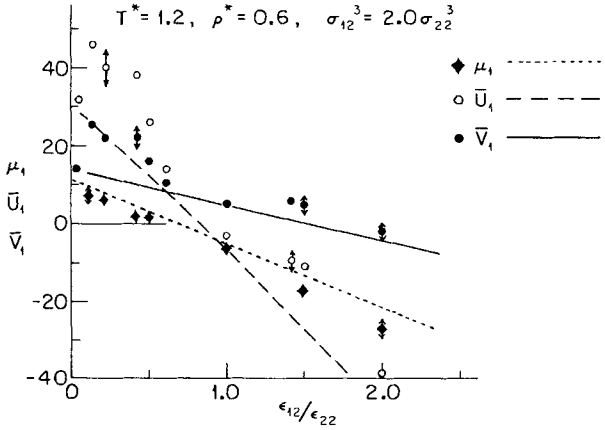

Figure 1b.

Figure 1. Partial molar properties as a function of ratio of Lennard-Jones energy parameters of solute-solvent interaction, $\epsilon_{12}/\epsilon_{22}$.

All partial molar properties at infinite dilution; superscripts ∞ and r (residual) omitted
μ_1, $\bar{U}_1$ reduced with respect to ϵ_{22}; $\bar{V}_1$ reduced with respect to σ_{22}^3
Curves: vdWI results; points: simulation results
Uncertainties not shown for all points to avoid crowding; see Table 1 for complete listing

solvent molecules have receded, and there is a resultant expansion. The important point to note in this figure is that even at liquidlike densities, g_{12} is not independent of ϵ_{12}.

In Figures 3a and 3b we show the density dependence of the infinite-dilution partial molar properties for a weakly interacting ($\epsilon_{12}/\epsilon_{22} = 0.5$) but large [$(\sigma_{12}/\sigma_{22})^3 = 3.5$] solute at two temperatures $T^* = 1.5$ and $T^* = 2.0$. The density dependences for the two temperatures are essentially qualitatively similar, except that the effects are much smaller at the higher temperature of $T^* = 2.0$. The chemical potential μ_1^∞ increases with density, which is as expected since it takes more work to create a cavity at high density and the weak ϵ_{12} implies that the entropic contributions dominate. $\bar{V}_1^\infty$ is positive and goes through a maximum at moderate densities. The positive $\bar{V}_1^\infty$ is due to the screening effect of a weakly attractive ($\epsilon_{12} = 0.5\epsilon_{22}$) and large ($\sigma_{12}^3 = 3.5\sigma_{22}^3$) solute mentioned in connection with Figure 1b. At low densities, the molecules are sufficiently far away from each other so that the effect of intermolecular forces is not significant, while at high densities, the liquid is incompressible. Consequently, $\bar{V}_1^\infty$ is moderate for both low and high densities. At moderate densities, the molecules are sufficiently close to be affected by intermolecular forces, and yet the fluid is still compressible. The screening effect of the weakly interacting large solute in this case causes a large expansion in volume. This does not occur to a comparable extent at the higher temperature of $T^* = 2.0$, which can be explained by noting the fact that $T^* = 1.5$ is sufficiently close to the critical temperature of $T^* = 1.36$ that the fluid is highly expandable, while $T^* = 2.0$ is quite supercritical and the large pressure serves to confine the fluid and as a result we do not see a large expansion. We can again examine the distribution functions for this model to see if they support the

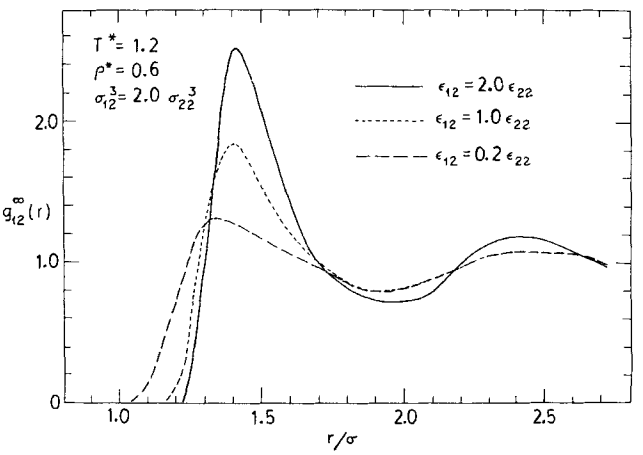

Figure 2. Infinite dilution g_{12} at three values of Lennard-Jones energy ratio for system of Figure 1b.

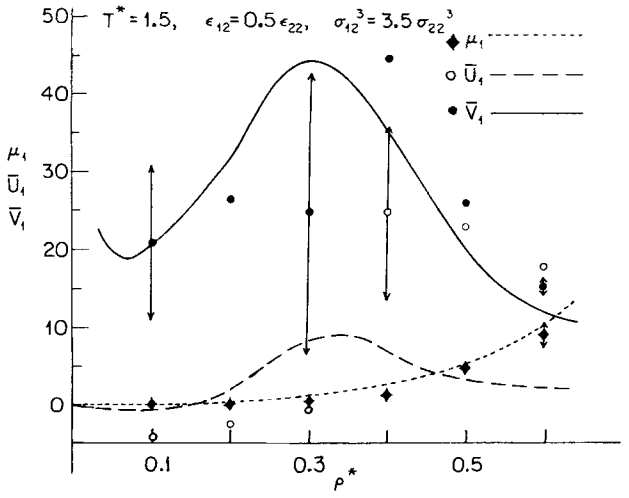

Figure 3a.

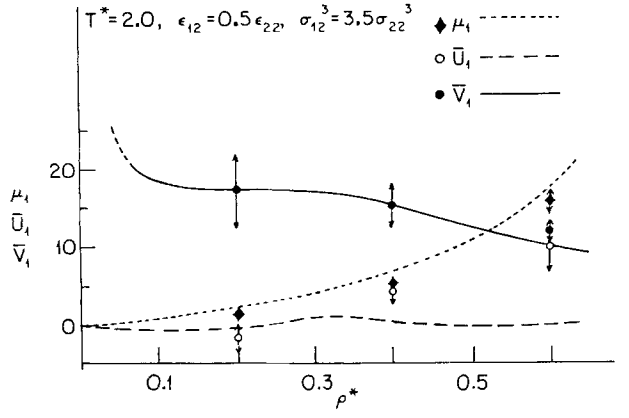

Figure 3b.

Figure 3. Infinite dilution partial molar properties as a function of density for weakly attractive large solute.

Curves: vdWI results; points: simulation results
See Table 2 for uncertainties on all simulation points

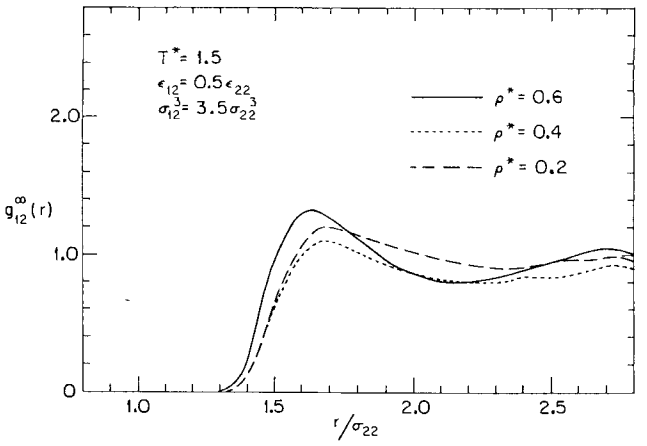

Figure 4. Infinite dilution g_{12} at three reduced densities ρ^* for weakly attractive large solute.

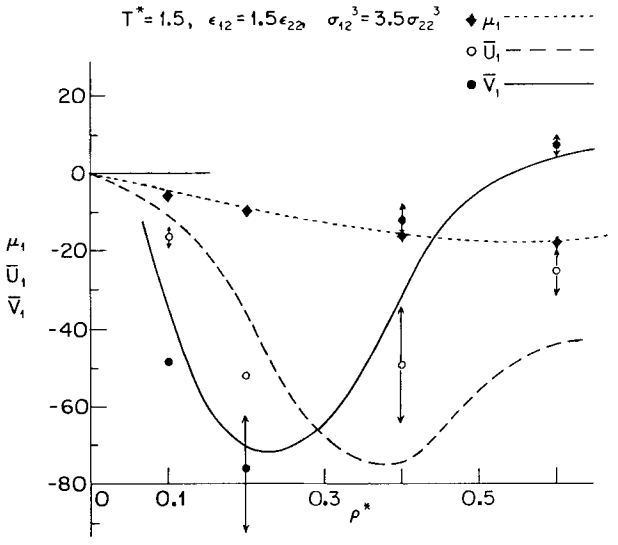

Figure 5a.

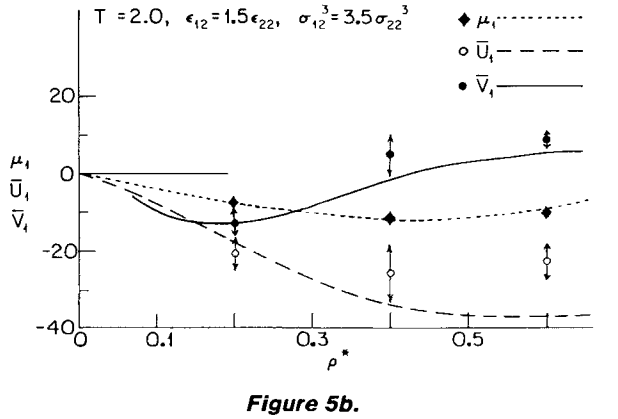

Figure 5b.

Figure 5. Infinite dilution partial molar properties as a function of density for strongly attractive large solute.

Curves: vdWI results; points: simulation results
See Table 2 for uncertainties on all simulation points

explanation given above. In Figure 4 we show the g_{12} for $T^* = 1.5$ at three different densities, $\rho^* = 0.2$, 0.4, and 0.6. We note that all three g_{12} have low peaks, reflective of the weak ϵ_{12}. Also we see that the g_{12} corresponding to $\rho^* = 0.4$ is the lowest of the three g_{12}'s, which is in agreement with the observed maximum in $\bar{V}_1^\infty$ at moderate densities shown in Figure 3a.

Figures 5a and 5b show the density dependence of the infinite-dilution partial molar properties at $T^* = 1.5$ and $T^* = 2.0$ for a large ($\sigma_{12}^3 = 3.5\sigma_{22}^3$) and strongly interacting ($\epsilon_{12} = 1.5\epsilon_{22}$) solute. Again the effects are much smaller at the higher temperature. The μ_1^∞ now decreases with increasing ρ^*. This is as expected since the shorter distances between molecules at higher densities result in an enhanced attraction, and the large ϵ_{12} means that the energetic contribution to the chemical potential now dominates over the entropic contribution. Therefore, the net result is a decrease in chemical potential with density. The $\bar{V}_1^\infty$ are in general negative except at high densities, where values are slightly positive. This is also as expected since the strong solute draws solvent molecules close to it and causes a reduction in

volume. At high densities, the liquid is incompressible and so we see a small positive $\bar{V}_1^\infty$. At low densities the reduction in volume is modest because the molecules are far apart. At moderate densities, the strong attraction of the solute coupled with the shorter distance between molecules and the fact that the fluid is moderately compressible, result in a minimum in $\bar{V}_1^\infty$ or a maximum reduction in volume. The corresponding distribution functions for three densities, $\rho^* = 0.2$, 0.4, and 0.6 at $T^* = 1.5$ are shown in Figure 6. We see indeed that the maximum volume reduction at $\rho^* = 0.2$ shown in Figure 5a corresponds to a large peak in g_{12} at $\rho^* = 0.2$. In fact g_{12} for $\rho^* = 0.2$ lies above curves for both $\rho^* = 0.4$ and $\rho^* = 0.6$. A comparison of Figures 4 and 6 shows that the density dependence of g_{12} depends on ϵ_{12} and is different from the pure solvent case, where the first peak in $g(r)$ always increases with ρ^*. In Figure 7 we show for reference purposes the $g(r)$ for pure solvent (Goldman, 1979) at $\rho^* = 0.2$, 0.4, and 0.6. Thus we can again anticipate that the density dependence of the van der Waals I mixing rules, which assume g_{12} to be independent of ϵ_{12} at infinite dilution, Eq. 8, will be inadequate.

Comparison with van der Waals I (vdWI) Theory

vdWI infinite-dilution partial molar properties for systems examined in simulation studies are shown as curves in Figures 1, 3, and 5 together with the simulation data. The Lennard-Jones equation of state of Nicholas et al. (1979) was used. Figure 1a shows the ϵ_{12} dependence at the liquid density of $\rho^* = 0.7$. We see that the vdWI results are linear in ϵ_{12} and do not reproduce the limiting values of zero for μ_1^∞, $\bar{U}_1^\infty$, and $\bar{V}_1^\infty$ at $\epsilon_{12} = 0$. The differences between vdWI and simulation results are smallest for μ_1^∞, followed by $\bar{V}_1^\infty$, and are largest for $\bar{U}_1^\infty$. For the state condition shown in Figure 1a, the differences for μ_1^∞ and $\bar{V}_1^\infty$ are within the simulation statistical uncertainties, while the differences for $\bar{U}_1^\infty$ are larger than the statistical uncertainties. The magnitudes of these differences in Figure 1b are much larger than those in Figure 1a because Figure 1b is for a state near the solvent phase boundary. Except for $\epsilon_{12}/\epsilon_{22}$ near unity, the differences between simulation and vdWI results are greater than the statistical uncertainties. This implies that when there is significant structural rearrangement due to introduction of a nonideal solute, the vdWI theory, which does not account for such structural perturbations, gives poor results.

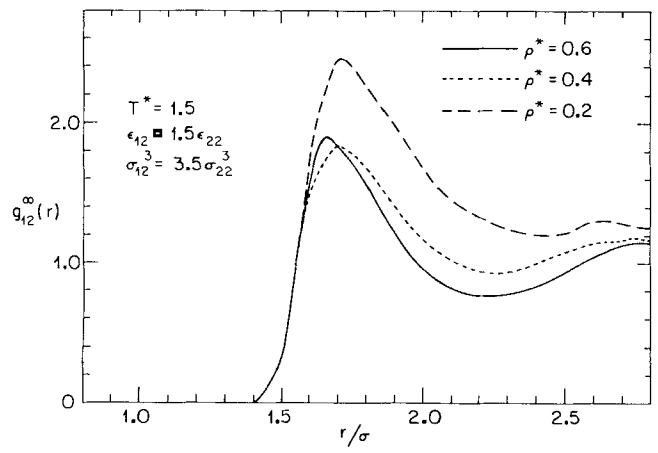

Figure 6. Infinite dilution g_{12} at three reduced densities ρ^* for strongly attractive large solute.

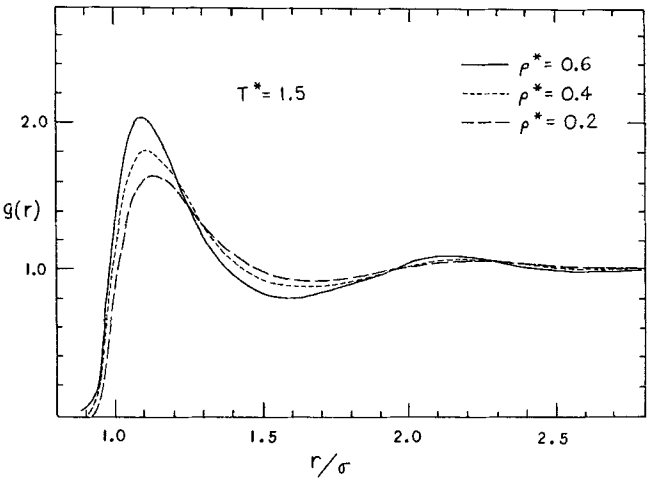

Figure 7. $g(r)$ for pure Lennard-Jones fluid at three reduced densities ρ^*, calculated using Goldman's fitted equations.

Results for the weakly interacting large solute and for the strongly interacting large solute are shown in Figures 3 and 5, respectively. The qualitative trends in μ_1^∞ are well represented by the vdWI theory, with the simulation μ_1^∞ being always lower than the corresponding vdWI values. Agreement is particularly good for the strongly interacting solute, Figure 5. This would imply that the vdWI theory is probably adequate for describing the attractive interactions but poor for repulsive interactions. For $\bar{U}_1^\infty$ and $\bar{V}_1^\infty$, the statistical uncertainties are large at the near-critical temperature of $T^* = 1.5$. Based on the comparisons shown in Figures 3 and 5, we conclude that given the large error bars on simulation results for $\bar{U}_1^\infty$ and $\bar{V}_1^\infty$, vdWI results for $\bar{U}_1^\infty$ and $\bar{V}_1^\infty$ seem satisfactory for most situations. This seems contradictory to the conclusion we arrived at based on study of the distribution functions, where we saw that the g_{12} in the mixture is quite different from the approximation of vdWI theory. The reason is perhaps the following: Since we are studying infinitely dilute systems, the properties are dominated by those of the solvent. We have seen that the partial molar properties are sensitive to the ease of compression/expansion of the mixture (or of the pure solvent in the case of infinite dilution). Since the equation of state accurately describes the properties of the pure solvent and in particular, the isothermal compressibility is well represented, the partial molar properties at infinite dilution are reasonably well represented. If the above reasoning is correct, then we cannot in general expect the same good representation at finite concentrations since the isothermal compressibility of a mixture according to vdWI at finite concentration is subject to approximations in the mixing rules and may not be close to the actual isothermal compressibility of the mixture. We are currently studying finite concentration cases to verify this.

Conclusions

We have presented infinite-dilution partial molar properties for Lennard-Jones mixtures and examined the density, temperature, and ϵ_{12} dependence of these properties. The structural information contained in the distribution functions is found to be valuable in interpreting and understanding the qualitative trends in the partial molar properties. We found that these prop-

erties are sensitive to the isothermal compressibility of the mixture. A brief comparison with vdWI theory was made. The qualitative description is in general reasonable except near phase boundaries. Since the simulation distribution function g_{12} is different from the approximate g_{12} according to the vdWI mixing rules, and the density dependence of the actual g_{12} is also different, we suspect that this reasonable agreement for partial molar properties is restricted to infinite-dilution cases. We conclude that structure information such as g_{12} provides an even more sensitive test of the mixing rules than the partial molar properties, and should be valuable in the development of improved mixing rules. Furthermore, since the partial molar properties are sensitive to the isothermal compressibility of the mixture, not only to the density, we should perhaps be developing compressibility-dependent mixing rules, rather than only density-dependent mixing rules.

Acknowledgment

This work was supported by the National Science Foundation, Grant No. CBT-8452001, and the Petroleum Research Fund, administered by the American Chemical Society, Grant No. 15350-G5. Support from Chevron Oilfield Research, La Habra, and from the Chevron Refinery, El Segundo, is gratefully acknowledged.

Notation

g = radial distribution function
g_{12} = radial distribution function of solute-solvent molecules
g_{22} = radial distribution function of solvent molecules
k = Boltzmann constant
N = number of molecules
N_1 = number of solute molecules
N_2 = number of solvent molecules
p = pressure
r = intermolecular separation
T^* = kT/ϵ_{22}, reduced temperature
U = internal energy
$\bar{U}_1^\infty$ = partial molar internal energy of solute at infinite dilution
V = volume
$\bar{V}_1^\infty$ = partial molar volume of solute at infinite dilution
x = mole fraction

Greek letters

ϵ_{12} = Lennard-Jones energy parameter of solute-solvent interaction
ϵ_{22} = Lennard-Jones energy parameter of solvent-solvent interaction
μ_1^∞ = chemical potential of solute at infinite dilution
$\mu_1'^\infty$ = residual chemical potential of solute at infinite dilution
$\mu_2'^0$ = pure solvent residual chemical potential
ξ = Kirkwood charging parameter
ρ^* = $(N/V)\sigma_{22}^3$ reduced density
σ_{12} = Lennard-Jones size parameter of solute-solvent interaction
σ_{22} = Lennard-Jones size parameter of solvent-solvent interaction
ψ_1 = energy experienced by a solute test particle
ψ_2 = energy experienced if the solute molecule were a solvent molecule
$\Delta\psi_1 = \psi_1 - \psi_2$

Appendix: Simulation Methods and Error Estimates

Simulation Methods

μ_1^∞ simulation

For $\rho^* < 0.6$, the test particle method in the canonical ensemble is used. 108 solvent particles are placed in a volume corresponding to the macroscopic density studied. Each simulation averages 1.5 million configurations after equilibrium. After every 108 configurations, 200 randomly placed solute test particles are brought into the simulation volume and the ensemble average in Eq. 1 is calculated.

For $\rho^* \geq 0.6$, the modified Kirkwood method in the isothermal-isobaric (NpT) ensemble is used. 107 solvent particles and a single coupled particle are placed in a volume corresponding to the macroscopic density of the state condition studied. The pressure is set at the value given by the Lennard-Jones equation of state (LJEOS) corresponding to the macroscopic density and system temperature. As the simulation proceeds, the system volume is adjusted according to the NpT ensemble probability distribution. The coupling parameter ξ is set at a value between 0 and 1. The ensemble average $\langle\Delta\psi_1\rangle_\xi$ in Eq. 2 is calculated. Since $\Delta\psi_1$ is an energy, reliable averages can be obtained in 0.5 million configurations. This value of $\langle\Delta\psi_1\rangle_\xi$ represents a single value of the integrand in Eq. 2. A series of between 10 and 20 simulations of this type for values of ξ in the interval [0, 1] is performed and the integral in Eq. 2 calculated. μ_1^∞ is found by adding the pure-solvent chemical potential $\mu_2'^0$ given by the LJEOS.

$\bar{U}_1^\infty$ and $\bar{V}_1^\infty$ simulation

$U(N_1 = 1, N_2, T, P)$ in Eq. 3 is the ensemble average internal energy of a system of one solute and 107 solvent particles at the specified pressure P and temperature T. This quantity is calculated as an NpT ensemble average with P set at the value given by the LJEOS corresponding to the required macroscopic density. The simulation also yields $V(N_1 = 1, N_2, T, P)$, which is the ensemble-averaged system volume. The average number of configurations is between 1 and 2 million per simulation. The longer simulations are for states at the lower temperature or near phase boundaries where the statistical fluctuations are larger.

$U(N_1 = 0, N_2, P, T)$ is given by $107 \times u$ where u is the internal energy per particle at the specified pressure and temperature given by the LJEOS.

$V(N_1 = 0, N_2, P, T)$ is given by $107/\rho^*$ where ρ^* is the macroscopic density at the specified P and T according to the LJEOS.

$\bar{U}_1^\infty$ and $\bar{V}_1^\infty$ are then found using Eqs. 3 and 4.

Uncertainty Estimate

Statistical fluctuations

The contribution of statistical fluctuations is the easiest to estimate. For each quantity to be averaged, subaverages over 100,000 configurations are recorded as well as the overall average. The root mean square deviation of the subaverages from the overall average is used as a measure of the statistical fluctuations. In the case of μ_1^∞ obtained using the modified Kirkwood method, where an integration of ensemble averages is required, we assumed that no systematic errors exist in the integrand so the quoted statistical fluctuations represent the average fluctuations in a typical integrand.

System size

Recent studies (Shing et al., 1988) have shown that there is no significant system size dependence in the simulated μ_1^∞ when N is changed from 108 to 256. it is difficult to estimate the system size dependence of $\bar{V}_1^\infty$ (and $\bar{U}_1^\infty$) without performing very time-consuming simulations. This is because $\bar{V}_1^\infty$ is calculated

using the equation

$$\bar{V}_1^{\infty} = V(N_1 = 1) - V(N_1 = 0)$$

where $\bar{V}_1^{\infty}$ is an intensive property of order 1, whereas $V(N_1 = 1)$ and $V(N_1 = 0)$ are both extensive properties and are of order N. As we increase the system size N, both $V(N_1 = 1)$ and $V(N_1 = 0)$ increase while their difference (which is $\bar{V}_1^{\infty}$) remains more or less constant. This means we are taking a (constant) difference of two increasingly large numbers. Furthermore, the magnitudes of the absolute statistical fluctuations in $V(N_1 = 1)$ and $V(N_1 = 0)$ also increase with N even though the statistical fluctuations relative to the mean decrease with N. As a result, simulations for large N are time-consuming not only because there are more particles, but because we also need to run more configurations in order to maintain the same size absolute statistical fluctuations. It would be interesting to study the N dependence of $\bar{U}_1^{\infty}$ and $\bar{V}_1^{\infty}$ although we did not do so in this work. We expect the effects to be negligible for low densities since the volumes are sufficiently large that if we consider the simulation cell to be centered on the single solute particle, the solute-solvent interactions would have become negligible at the cutoff, and the structure of the fluid outside the cutoff point is essentially that of the unperturbed pure solvent. For higher densities, the volumes are smaller so that the solute-solvent interactions may still be significant at the cutoff point and the usual tail corrections underestimate the contributions beyond the cutoff. So we expect, in general, the magnitudes of $\bar{V}_1^{\infty}$ and $\bar{U}_1^{\infty}$ to be greater for larger systems because a larger cutoff can be used.

Lennard-Jones equation of state (LJEOS):

The accuracy of the LJEOS affects the uncertainties in $\bar{V}_1^{\infty}$, $\bar{U}_1^{\infty}$, and μ_1^{∞} calculated using the Kirkwood method because the quantities $U(N_1 = 0)$, $V(N_1 = 0)$, and $\mu_2'^0$ in Eqs. 3–5 are obtained using the LJEOS. μ_1^{∞} results found by using the test particle method are not affected. By comparing the $U(N_1 = 0)$ and $V(N_1 = 0)$ and $\mu_2'^0$ values given by the LJEOS with actual selected simulation results, we found that the internal energies $U(N_1 = 0)$ differ by less than 1%, and the volumes $V(N_1 = 0)$ and $\mu_2'^0$ differ by about 1%. This means that the LJEOS contribution to the total uncertainties is at the maximum comparable to that from the statistical fluctuations. In many cases, especially where the magnitudes of the partial molar properties are large, the LJEOS contribution is much less. Therefore, the total uncertainties from these two sources are at most twice the uncertainties cited in Tables 1–3. We only quote the uncertainties due to statistical fluctuations in Tables 1–3 because we believe that the LJEOS-derived uncertainties have little effect on the qualitative trends observed here. For example, the statistical fluctuations affect the accuracy of the simulated values of $V(N_1 = 1)$, $U(N_1 = 1)$, and $\int \langle \Delta\psi_1 \rangle_{\xi} d\xi$, while the uncertainties in the LJEOS affect the accuracy of $U(N_1 = 0)$, $V(N_1 = 0)$, and $\mu_2'^0$, which are either added to or subtracted from the corresponding $N_1 = 1$ quantities in order to obtain the partial molar properties. In many cases (for example, the results shown in Table 1), the same $N_1 = 0$ values are added or subtracted for the various $\epsilon_{12}/\epsilon_{22}$ ratios so that the observed trend in the variation with $\epsilon_{12}/\epsilon_{22}$ should be independent of the uncertainties in the LJEOS.

Literature Cited

Debenedetti, P. G., "Derivation of Operational Definitions for the Computer Calculation of Partial Molar Properties in Multicomponent Mixtures," *Chem. Phys. Lett.*, **132,** 325 (1986).

Eckert, C., D. H. Ziger, K. P. Johnston, and S. Kim, "Solute Partial Molal Volumes in Supercritical Fluids," *J. Phys. Chem.*, **90,** 2738 (1986).

Goldman, S., "An Explicit Equation for the Radial Distribution Function of a Dense Lennard-Jones Fluid," *J. Phys. Chem.*, **83,** 3033 (1979).

Leland, T. W., J. S. Rowlinson, and G. A. Sather, "Statistical Thermodynamics of Mixtures of Molecules of Different Sizes," *Trans. Farad. Soc.*, **64,** 1447 (1968).

McDonald, I. R., *Statistical Mechanics*, **1,** K. Singer, ed., Specialist Periodical Reports, Chemical Society, London (1973).

Nicholas, J. J., K. E. Gubbins, W. B. Streett, and D. J. Tildesley, "Equation of State for the Lennard-Jones Fluid," *Molec. Phys.*, **37,** 1429 (1979).

Shing, K. S., and S. T. Chung, "Computer Simulation Methods for the Calculation of Solubility in Supercritical Extraction Systems," *J. Phys. Chem.*, **91,** 1674 (1987).

Shing, K. S., and K. E. Gubbins, "The Chemical Potential from Computer Simulation Test Particle Method with Umbrella Sampling," *Molec. Phys.*, **43,** 717 (1981).

———, "The Chemical Potential in Dense Fluids and Fluid Mixtures via Computer Simulation," *Molec. Phys.*, **46,** 1109 (1982).

Shing, K. S., K. E. Gubbins, and K. Lucas, "Henry Constants in Nonideal Fluid Mixtures, Computer Simulation and Theory," preprint (1988).

Widom, B., "Some Topics in the Theory of Fluids," *J. Chem. Phys.*, **39,** 2808 (1963).

Manuscript received Feb. 9, 1987, and revision received July 13, 1988.